IOPscience iopscience.iop.org

Home Search Collections Journals About Contact us My IOPscience

Fabrication and Characterization of High-Mobility Graphene p–n–p Junctions Encapsulated by Hexagonal Boron Nitride

This content has been downloaded from IOPscience. Please scroll down to see the full text.

2013 Jpn. J. Appl. Phys. 52 110105

(http://iopscience.iop.org/1347-4065/52/11R/110105)

View the table of contents for this issue, or go to the journal homepage for more

Download details:

IP Address: 129.120.87.225
This content was downloaded on 07/02/2017 at 17:13

Please note that terms and conditions apply.

You may also be interested in:

Fabrication of p–n–p Graphene Structure and Observation of Current Oscillation
Keita Konishi and Kanji Yoh

Formation of Graphene-on-Diamond Structure by Graphitization of Atomically Flat Diamond (111) Surface
Norio Tokuda, Makoto Fukui, Toshiharu Makino et al.

Towards Graphene GHz/THz Nanosensor
Akram M. Mahjoub, Shoutaro Motooka, Nobuyuki Aoki et al.

Gate-Controlled P–I–N Junction Switching Device with Graphene Nanoribbon
Shu Nakaharai, Tomohiko Iijima, Shinichi Ogawa et al.

Electrical Spin Injection into Graphene through Monolayer Hexagonal Boron Nitride
Takehiro Yamaguchi, Yoshihisa Inoue, Satoru Masubuchi et al.

Dependence of Field-Effect Mobility of Graphene Grown by Thermal Chemical Vapor Deposition on Its Grain Size
Katsunori Yagi, Ayaka Yamada, Kenjiro Hayashi et al.

Density-of-States Limited Contact Resistance in Graphene Field-Effect Transistors
Kosuke Nagashio and Akira Toriumi

Room Temperature Logic Inverter on Epitaxial Graphene-on-Silicon Device
Amine El Moutaouakil, Hyun-Chul Kang, Hiroyuki Handa et al.

Electrical transport in high-quality graphene pnp junctions
Jairo Velasco Jr, Gang Liu, Wenzhong Bao et al.

Japanese Journal of Applied Physics **52** (2013) 110105
http://dx.doi.org/10.7567/JJAP.52.110105

Fabrication and Characterization of High-Mobility Graphene p–n–p Junctions Encapsulated by Hexagonal Boron Nitride

Satoru Masubuchi[1,2*], Sei Morikawa[1], Masahiro Onuki[1], Kazuyuki Iguchi[1], Kenji Watanabe[3], Takashi Taniguchi[3], and Tomoki Machida[1,2*]

[1] *Institute of Industrial Science, University of Tokyo, Meguro, Tokyo 153-8505, Japan*
[2] *Institute for Nano Quantum Information Electronics, University of Tokyo, Meguro, Tokyo 153-8505, Japan*
[3] *National Institute for Materials Science, Tsukuba, Ibaraki 305-0044, Japan*
E-mail: msatoru@iis.u-tokyo.ac.jp; tmachida@iis.u-tokyo.ac.jp

Received May 1, 2013; accepted August 8, 2013; published online October 22, 2013

We report on the fabrication and characterization of high quality graphene p–n–p junctions encapsulated by hexagonal boron nitride. By tuning the back gate and top gate bias voltages, a graphene p–n–p junction with tunable polarity and doping levels was realized. The p–n–p junction displayed distinct resistance oscillations, which was attributed to the Fabry–Perot interference of charge carriers in the p–n–p cavity. When a small magnetic field was applied, the oscillation phase was shifted by π, indicating the observation of Klein tunneling of charge carriers in the p–n–p junctions. The observation of Fabry–Perot interference and Klein tunneling with a macroscopic cavity length of $L_c = 500$ nm demonstrates the markedly high quality of our graphene p–n–p junction. © 2013 The Japan Society of Applied Physics

1. Introduction

Owing to a linear energy dispersion relation, charge carriers in graphene behave as massless Dirac fermions,[1)] and the presence of Dirac fermions leads to the observation of novel transport phenomena such as the half integer quantum Hall effect[2,3)] and an unusual sequence in the fractional quantum Hall effect.[4,5)] When the charge carrier phase coherence length becomes comparable to the sample size, charge carriers exhibit interference phenomena such as the Aharanov–Bohm effect.[6)] In particular, when charge carriers are confined within p–n–p junctions, Dirac fermions exhibit novel transport phenomena such as Fabry–Perot oscillations[7)] and Klein tunneling.[8–10)] Because of the uniqueness of these transport phenomena, graphene p–n–p junctions are expected to serve as a new platform for developing device applications with new functionality,[11)] such as an electron beam splitter[12)] and a Veselago lens.[12,13)]

Graphene p–n–p junctions have typically been fabricated using double-gated graphene with an oxide gate dielectric.[8,10,14–17)] However, the presence of the gate dielectric proximity to graphene induces additional charge carrier scattering sources in graphene.[16,18)] As a result, the charge carrier mean free path l_{mfp} was limited to ~100 nm,[16)] thus small device structures of ~20 nm in length were required to observe phase coherent transport phenomena.[10)] Suspended graphene has a large carrier mean free path of $l_{mfp} \sim 1$ μm,[19,20)] however, the requirement for suspended gate structure severely limited device geometries.[21)] Recent developments in the mechanical transfer technique of graphene on atomically flat hexagonal boron nitride (h-BN) flakes have enabled the fabrication of high quality substrate-supported graphene.[22)] From the viewpoint of device fabrication technology, substrate-supported structure is suitable for studying phase coherent transport phenomena because it provides better degree of freedom in device geometries. The recent experimental studies reported fabrication of tri-layer graphene p–n–p junctions and observation of Fabry–Perot oscillation.[23)] However, in this case the junction length was ~60 nm. Moreover, the characteristic transport phenomena of massless Dirac fermions such as Klein tunneling were not observed. Thus, the fabrication and characterization of monolayer graphene p–n–p junctions encapsulated by hexagonal boron nitride still remains to be demonstrated.

In this paper, we report on the fabrication and characterization of high quality graphene p–n–p junctions encapsulated by h-BN. Our h-BN encapsulated graphene showed a high mobility of $\mu \sim 100{,}000\,\mathrm{cm^2\,V^{-1}\,s^{-1}}$ at $T = 1.6$ K. By tuning the back gate and top gate bias voltages, graphene p–n–p junctions with tunable polarity and doping levels were formed. In these p–n–p junctions, we observed distinct resistance oscillations, which were attributed to the Fabry–Perot interference of charge carriers within the p–n–p cavity. When a small magnetic field was applied, the oscillation phase was shifted by π, indicating the observation of Klein tunneling of charge carriers within the p–n–p junctions. The observation of Fabry–Perot oscillations and Klein tunneling over the macroscopic cavity length of $L_c = 500$ nm demonstrates the markedly high quality of our graphene p–n–p junctions. These results indicate graphene/h-BN heterostructures provide a suitable platform for investigating novel charge carrier transport phenomena of Dirac fermions in graphene.

2. Experimental Methods

Figure 1 shows a schematic and atomic force microscopy (AFM) image of the device studied in this work. First, we deposited a ~50-nm-thick h-BN flake by mechanical exfoliation of h-BN on a Si wafer with a thermally oxidized layer of 290-nm-thick SiO_2. Monolayer graphene flakes were then deposited on a separate Si wafer with a spin-coated poly(methyl methacrylate) (PMMA) layer. The graphene on the PMMA layer was transferred to the h-BN crystal using an alignment technique under an optical microscope.[22,24)] The graphene on h-BN was then encapsulated by a 10-nm-thick h-BN flake using the mechanical transfer technique. We annealed the sample in Ar–H_2 (97 : 3) gas flow at $T = 350\,^\circ$C for 5 h to remove any residue induced by the transfer process. Finally, the top gate (TG) and electrical contacts were defined by electron beam lithography followed by the evaporation of Pd (80 nm) and

 © 2013 The Japan Society of Applied Physics

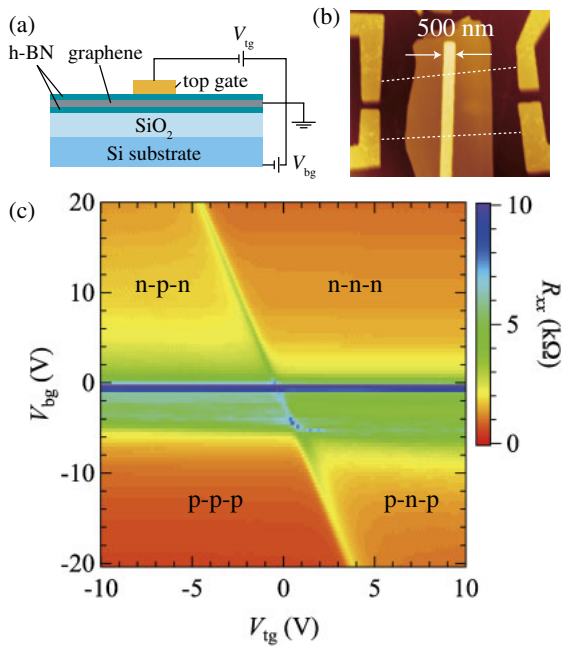

Fig. 1. (Color online) (a) Schematic of our device. A local top gate is fabricated on h-BN-encapsulated monolayer graphene. A heavily doped Si bottom gate changes the charge carrier density throughout the whole flake, whereas the top gate affects only the gated region. By tuning the gate bias voltages, carriers with different types can be induced in locally gated regions from the rest of sample. (b) AFM image of the device studied in this work. White dashed lines indicate edges of the graphene flake. The length of the top gate electrode is $L_c = 500$ nm. (c) Color plot of four-terminal resistance as a function of top gate (V_{tg}) and back gate (V_{bg}) bias voltages measured at $T = 1.6$ K.

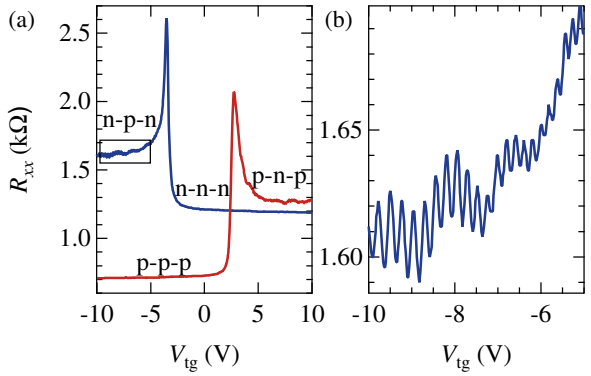

Fig. 2. (Color online) (a) Resistance R_{xx} as a function of top gate voltage V_{tg} at $V_{bg} = -15$ V (red) and 15 V (blue). (b) Expanded view of R_{xx} as a function of V_{tg} in the area surrounded by solid rectangle in (a).

lift-off. The resist residues were removed by annealing the sample in Ar–H_2 (97 : 3) gas flow at $T = 300\,^{\circ}$C for 6 h. The length of the top gate was $L_c = 500$ nm. The measurements were performed in a ^{4}He-cooled variable temperature insert at temperatures $T = 1.5$–300 K. Transport measurements were carried out using a standard lock-in technique with a small alternating current of $I_{ac} = 100$ nA. Magnetic fields were applied perpendicularly to the sample surface using a superconducting magnet.

To tune the charge carrier density, a heavily doped Si substrate was used as a global back gate, V_{bg}, and a local top metal electrode was used as a local top gate, V_{tg}. The charge carrier density in the top gated region was tuned according to the relation $n_1 = C_{tg}(V_{tg} - V_{D,tg}) + C_{bg}(V_{bg} - V_{D,tg})$, where C_{tg} is the capacitance between graphene and the top gate, C_{bg} is the capacitance between graphene and the back gate. $V_{D,tg}$ and $V_{D,bg}$ are the values of V_{tg} and V_{bg}, corresponding to the charge neutrality points for the top gated and non-top gated regions. The charge carrier density in the bare region (non-top gated region) was modulated according to $n_2 = C_{bg}(V_{bg} - V_{D,bg})$. Thus, by tuning V_{bg} and V_{tg}, graphene junctions with different charge carrier densities n_2–n_1–n_2 were formed. Our h-BN-encapsulated device shows low disorder, with a high mobility of $\mu = 100{,}000\,\mathrm{cm^2\,V^{-1}\,s^{-1}}$ at $T = 1.6$ K.

3. Results and Discussion

For the characterization of the device, we measured the four-terminal resistance R_{xx} as a function of V_{bg} and V_{tg}, as shown in Fig. 1(c). We observed resistance peak structures running horizontally and diagonally in Fig. 1(c). The horizontal line is independent of top gate bias voltage, and thus corresponds to the charge neutrality point in the non-gated region. The diagonal line is dependent on V_{tg} and V_{bg}, which corresponds to the charge neutrality point in the top gated region. The slope yields the capacitance ratio $\eta = C_{tg}/C_{bg} \sim 5.0$. This ratio is in agreement with the value obtained by geometrical considerations $C_{tg}/C_{bg} = \epsilon_{tg}d_{bg}/\epsilon_{bg}d_{tg} \sim 5.5$, where ϵ is the gate dielectric constant and d is the graphene-gate separation. The resistance map was partitioned into four regions by resistance maxima. These observations are qualitatively consistent with previous experimental studies on double gated graphene devices utilizing metal oxide gate dielectrics,[25] and demonstrates the formation of graphene p–n–p, n–p–n, n–n–n, and p–p–p junctions.

Here, we focus on the transport properties of p–n–p and n–p–n configurations, which are positioned in the top left part and lower right part of Fig. 1(c). In Fig. 2(a), we show R_{xx} as a function of V_{tg} at $V_{bg} = -15$ V (blue curve) and $V_{bg} = 15$ V (red curve). When junctions are in the bipolar regime p–n–p (n–p–n), the value of R_{xx} becomes higher than that for the unipolar regime p–p–p (n–n–n). The increased value of resistance is attributed to charge carrier scattering at the p–n interface, thus a graphene p–n–p junction forms charge carrier cavity. When the value of R_{xx} was more closely scrutinized in Fig. 2(a), the oscillation of R_{xx} as a function of V_{tg} was resolved [Fig. 2(b)]. In graphene/SiO_2 devices, this type of resistance oscillation in graphene p–n–p junctions was attributed to the Fabry–Perot interference of charge carriers between p–n interfaces.[10] A charge carrier gains a phase of $\Delta\phi$ as it travels across the p–n interface. When the accumulated phase becomes π, a standing wave forms from the interference between charge carriers moving forward and backward. The charge carriers entering perpendicular to the p–n–p junction do not contribute to interference due to Klein tunneling, the value obtained from the theoretical estimate reproduces the oscillation period in Fig. 2(b).[25,28] These observations indicate that the resistance oscillations in Fig. 2(b) can be attributed to the Fabry–Perot interference of charge carriers in graphene p–n–p junctions.

Here, we discuss the temperature dependence of Fabry–Perot oscillations. Figure 3(a) shows R_{xx} as a function of V_{tg}

© 2013 The Japan Society of Applied Physics

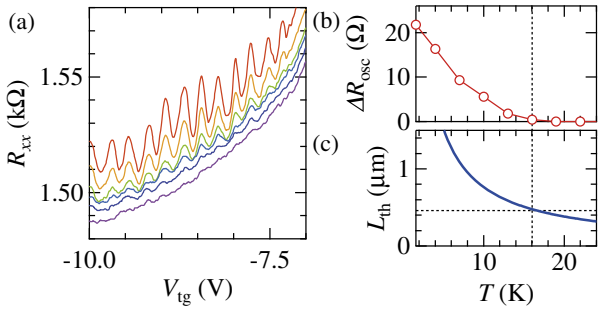

Fig. 3. (Color online) (a) R_{xx} as a function of V_{tg} for $T = 4$, 7, 10, 13, 16, and 19 K (top to bottom). (b) Oscillation amplitude ΔR_{osc} as a function of T. (c) Thermal length L_{th} as a function of T.

for temperatures $T = 4$, 7, 10, 13, 16, and 19 K. When the temperature was raised from $T = 1.6$ K, the oscillation amplitude gradually decreased until disappearing at $T = 19$ K. This behavior was summarized by plotting the oscillation amplitude ΔR_{osc} as a function of T in Fig. 3(b). In general, the condition for the emergence of phase coherent transport is $L_c < L_{th}$, L_{mfp}, where $L_{th} = hv_F/2\pi k_B T$ is the thermal length and L_{mfp} is the charge carrier mean free path. In Fig. 3(c), we plot the value of L_{th}. When the value of L_{th} becomes comparable to the cavity length $L_c = 500$ nm, the amplitude of resistance oscillations was reduced to zero [dotted lines in Figs. 3(b) and 3(c)], suggesting that the observation of Fabry–Perot oscillations at high temperature was limited by the thermal length L_{th}.

In previous experiments in conventional graphene on SiO_2,[10] the observation of Fabry–Perot oscillations and Klein tunneling required very small cavity lengths of $L_c = 20$ nm, because the charge carrier mean free path was limited to $L_{mfp} < 100$ nm. On the other hand, our graphene/h-BN showed Fabry–Perot oscillations with a cavity length of $L_c = 500$ nm. These observations demonstrate the markedly high quality of our graphene/h-BN junctions, which are an ideal platform for investigating electron-optics based transport phenomena, such as negative refraction index,[13] Veselago lensing, and electron beam switching,[12] because, the fabrication of multi-terminal and large size device structures are required to investigate these phenomena.

Finally, we demonstrate that the presence of phase coherent transport allows us to study the characteristic transport phenomena of Dirac fermions, namely the transmission of charge carriers through a potential barrier with unit probability. This phenomenon is known as Klein tunneling,[26–28] and has been demonstrated in double-gated graphene on SiO_2.[10] In Fig. 4(a), we show R_{xx} as a function of V_{tg} measured for magnetic fields of $B = 0$, 20, 40, 60, 80, and 100 mT [bottom to top]. When the magnetic field was increased from zero to $B = 20$ mT, the oscillation phase of R_{xx} was unchanged. As the magnetic field was increased further, to $B = 40$–60 mT, the peak positions were shifted to larger $|V_{tg}|$ as indicated by the black arrows in Fig. 4(a). For further increasing magnetic field, the peak positions were gradually shifted to larger $|V_{tg}|$. Finally, at $B = 100$ mT, the resistance peak positions become located at the positions of resistance minima for zero magnetic fields. This situation is more clearly indicated by plotting R_{xx} as a function of V_g and B in a two-dimensional color plot in Fig. 4(b). These

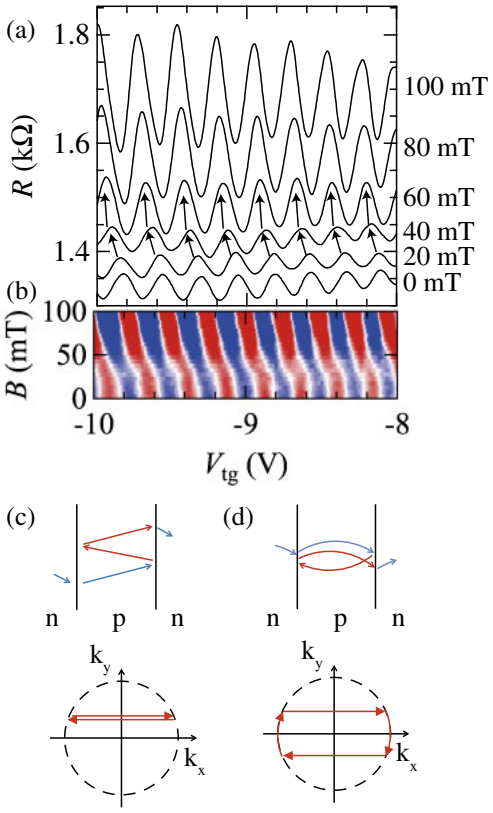

Fig. 4. (Color online) (a) R_{xx} as a function of V_{tg} measured for $B = 0$, 20, 40, 60, 80, and 100 mT (bottom to top) at $V_g = 15$ V. (b) Color plot of R_{xx} as a function of V_{tg} and B measured at $T = 1.6$ K. (c, d) Trajectories of charge carriers interfering within n–p–n junctions shown in real space (top) and reciprocal space (bottom) for $B = 0$ (c) and $B > B^*$ (d).

observations indicate that the oscillation phase of the Fabry–Perot resonance was shifted by π at a specific magnetic field of $B^* = 40$–60 mT.

The observed shift of the Fabry–Perot oscillation phase is explained within the framework of phase coherent transport and Klein tunneling in graphene p–n–p junctions.[26–28] At $B = 0$, the presence of perfect transmission prohibits charge carriers entering perpendicularly to the p–n junction to contribute to Fabry–Perot interference. Instead, charge carriers moving back and forth with oblique incident angle induce Fabry–Perot interference, whose trajectory in real and reciprocal space was illustrated in Figs. 4(c) and 4(d). When a magnetic field is applied, the charge carrier trajectories are bent by cyclotron motion, and when the magnetic field reaches a critical value of B^* as follows:

$$B^* = 2\hbar k_y / e L_c, \tag{1}$$

the trajectory in reciprocal space encloses the singularity point at $(k_x, k_y) = (0, 0)$ [Fig. 4(d)]. Thus, the charge carriers obtain an additional Berry's phase of π. As a result, the Fabry–Perot interference period was shifted by π. Based on Eq. (1), the value of B^* is estimated to be $B^* \sim 50$ mT. This value is in good agreement with the experimental data obtained in Fig. 4(b). These observations demonstrate the observation of Klein tunneling within our p–n–p junctions and that our graphene p–n–p junctions can be utilized as a platform for studying novel transport phenomena of Dirac fermions in monolayer graphene.

© 2013 The Japan Society of Applied Physics

4. Conclusions

To summarize, using hexagonal boron nitride as a gate dielectric layer, we fabricated graphene p–n–p junctions and conducted transport measurements. In these p–n–p junctions, we observed distinct resistance oscillations, which were attributed to the Fabry–Perot interference of charge carriers within the p–n–p cavity. When a small magnetic field was applied, the oscillation phase was shifted by π, indicating the observation of Klein tunneling of charge carriers in p–n–p junctions. The length of the p–n–p junction was $L_c = 500$ nm, which was an order of magnitude larger than that previously obtained using conventional graphene on a SiO_2 substrate.[10] This experiment indicates that graphene/h-BN p–n–p junctions can be utilized as a platform for investigating the transport phenomena of Dirac fermions, such as negative refraction index, Veselago lensing, and electron beam switching, which require extremely clean graphene devices.

Acknowledgements

The authors acknowledge R. Moriya for technical support and helpful discussions. This work was supported by the PRESTO, Japan Science and Technology Agency, the Special Coordination Funds for Promoting Science and Technology, Grant-in-Aid for Scientific Research from the the Ministry of Education, Culture, Sports, Science and Technology, and the CREST, Japan Science and Technology Agency.

1) A. K. Geim and K. S. Novoselov: Nat. Mater. **6** (2007) 183.
2) K. S. Novoselov, A. K. Geim, S. V. Morozov, D. Jiang, M. I. Katsnelson, I. V. Grigorieva, S. V. Dubonos, and A. A. Firsov: Nature **438** (2005) 197.
3) Y. Zhang, Y.-W. Tan, H. L. Stormer, and P. Kim: Nature **438** (2005) 201.
4) X. Du, I. Skachko, F. Duerr, A. Luican, and E. Y. Andrei: Nature **462** (2009) 192.
5) K. I. Bolotin, F. Ghahari, M. D. Shulman, H. L. Stormer, and P. Kim: Nature **462** (2009) 196.
6) S. Russo, J. Oostinga, D. Wehenkel, H. Heersche, S. Sobhani, L. Vandersypen, and A. Morpurgo: Phys. Rev. B **77** (2008) 085413.
7) F. Miao, S. Wijeratne, Y. Zhang, U. C. Coskun, W. Bao, and C. N. Lau: Science **317** (2007) 1530.
8) N. Stander, B. Huard, and D. Goldhaber-Gordon: Phys. Rev. Lett. **102** (2009) 026807.
9) E. Rossi, J. H. Bardarson, P. W. Brouwer, and S. Das Sarma: Phys. Rev. B **81** (2010) 121408.
10) A. F. Young and P. Kim: Nat. Phys. **5** (2009) 222.
11) S. Sutar, E. S. Comfort, J. Liu, T. Taniguchi, K. Watanabe, and J. U. Lee: Nano Lett. **12** (2012) 4460.
12) V. V. Cheianov, V. Fal'ko, and B. L. Altshuler: Science **315** (2007) 1252.
13) V. V. Cheianov and V. I. Fal'ko: Phys. Rev. B **74** (2006) 041403.
14) S. Kim, J. Nah, I. Jo, D. Shahrjerdi, L. Colombo, Z. Yao, E. Tutuc, and S. K. Banerjee: Appl. Phys. Lett. **94** (2009) 062107.
15) H. Miyazaki, K. Tsukagoshi, A. Kanda, M. Otani, and S. Okada: Nano Lett. **10** (2010) 3888.
16) K. Zou, X. Hong, D. Keefer, and J. Zhu: Phys. Rev. Lett. **105** (2010) 126601.
17) N. Gu, M. Rudner, A. Young, P. Kim, and L. Levitov: Phys. Rev. Lett. **106** (2011) 066601.
18) J.-H. Chen, C. Jang, S. Xiao, M. Ishigami, and M. S. Fuhrer: Nat. Nanotechnol. **3** (2008) 206.
19) X. Du, I. Skachko, A. Barker, and E. Y. Andrei: Nat. Nanotechnol. **3** (2008) 491.
20) K. I. Bolotin, K. J. Sikes, Z. Jiang, M. Klima, G. Fudenberg, J. Hone, P. Kim, and H. L. Stormer: Solid State Commun. **146** (2008) 351.
21) A. L. Grushina, D.-K. Ki, and A. F. Morpurgo: Appl. Phys. Lett. **102** (2013) 223102.
22) C. R. Dean, A. F. Young, I. Meric, C. Lee, L. Wang, S. Sorgenfrei, K. Watanabe, T. Taniguchi, P. Kim, K. L. Shepard, and J. Hone: Nat. Nanotechnol. **5** (2010) 722.
23) L. C. Campos, A. F. Young, K. Surakitbovorn, K. Watanabe, T. Taniguchi, and P. Jarillo-Herrero: Nat. Commun. **3** (2012) 1239.
24) S. Masubuchi, K. Iguchi, T. Yamaguchi, M. Onuki, M. Arai, K. Watanabe, T. Taniguchi, and T. Machida: Phys. Rev. Lett. **109** (2012) 036601.
25) J. Velasco, G. Liu, L. Jing, P. Kratz, H. Zhang, W. Bao, M. Bockrath, and C. N. Lau: Phys. Rev. B **81** (2010) 121407.
26) M. I. Katsnelson, K. S. Novoselov, and A. K. Geim: Nat. Phys. **2** (2006) 620.
27) A. Shytov, M. Rudner, and L. Levitov: Phys. Rev. Lett. **101** (2008) 156804.
28) A. F. Young and P. Kim: Annu. Rev. Condens. Matter Phys. **2** (2011) 101.

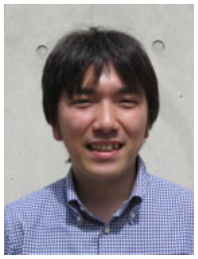

Satoru Masubuchi received the Ph. D. degrees in applied physics from the University of Tokyo in 2010. Since 2010 he has been an assistant Professor in the Institute for Nano Quantum Information Electronics, University of Tokyo. His current research interest includes quantum transport in graphene.

Masahiro Onuki received the M.E. degree in applied physics from the University of Tokyo in 2013. He was researching quantum transport in graphene/h-BN heterostructures.

Sei Morikawa received the B.E. degree in applied physics from the University of Tokyo in 2012. His current research interest includes quantum transport in graphene/h-BN heterostructures and their applications.

Kazuyuki Iguchi received the M.E. degree in applied physics from the University of Tokyo in 2012. He was researching quantum transport in graphene/h-BN heterostructures.

© 2013 The Japan Society of Applied Physics

Kenji Watanabe is a member of Environment and Energy Materials Division at National Institute for Materials Science (NIMS), where he serves as a chief researcher of Optoelectronic Materials Group in Optical and Electronic Materials Unit, pursuing the research for wide bandgap materials. He completed doctoral course (Physics) in faculty of Science at Hokkaido University (1990), joined Oki Electric Industry Co., Ltd. from 1990 to 1994, worked on the development of devices for optical fiber communication systems. He joined National Institute for Research in Inorganic Materials (NIRIM) from 1994. NIRIM was reorganized into NIMS in 2001.

Takashi Taniguchi received the B.S. degrees from Tokyo University of Agriculture and Technology in 1982, M.S., and Dr. Eng. degrees from Tokyo Institute of Technology (TIT), in 1984 and 1987, respectively. From 1987 to 1989, he joined TIT as a research associate. Since 1989 he has been working in National Institute for Materials Science. His current research field covers materials synthesis under high pressure.

Tomoki Machida received the Ph. D. degree from the University of Tokyo in 1998. Since 2004 he has been an associate Professor in the Institute of Industrial Science, University of Tokyo. His current research interests include quantum transport in low-dimensional electron systems and their applications.

© 2013 The Japan Society of Applied Physics